Characterisation of Dentatorubrothalamic tract with Diffusion Spectrum Imaging in Patients suffering from Parkinson's disease

Panagiotis N Papageorgiou (panagiotis.papageorgiou@uhs.nhs.uk)
University Hospital Southampton https://orcid.org/0000-0001-8696-4457
Frederic Rossi-mossuti
CHUV: Centre Hospitalier Universitaire Vaudois
Roland Wiest
Inselspital University Hospital Bern: Inselspital Universitatsspital Bern
Claus Kiefer
Inselspital University Hospital Bern: Inselspital Universitatsspital Bern
Martin Zbinden
Inselspital University Hospital Bern: Inselspital Universitatsspital Bern
Claudio Pollo
Inselspital University Hospital Bern: Inselspital Universitatsspital Bern

Research Article

Keywords: Dentatorubrothalamic tract, diffusion spectrum imaging, deep brain stimulation, fiber tracking, tremor, Parkinson's disease

Posted Date: June 7th, 2021

DOI: https://doi.org/10.21203/rs.3.rs-302260/v1

Abstract

Introduction: Clinical data support that the dentatorubrothalamic tract (DRTT) is an effective target for deep brain stimulation (DBS) in medically refractory tremor. Nevertheless, the achievement of a realistically detailed depiction of DRTT for preoperative direct targeting remains a challenge.

Methods: Ten patients with Parkinson's disease from the Inselspital Bern database were selected. We used diffusion spectrum imaging (DSI) scans for deterministic fiber tracking of the DRTT with the Track Vis software. Thereafter we compared our DSI-characterized DRTT with the existing anatomical data.

Results: In 6 out of 10 individuals the full course of DRTT has been in high affiliation/consistency/association/adherence with the anatomical course of DRTT as described in literature.

Conclusions: In this study DSI fiber tracking was used to characterize successfully the DRTT anatomical course in its complexity in a quest of the optimal DBS target for parkinsonian tremor. To our knowledge such attempt has not occurred before. Further studies are required to standardize the protocol of DRTT fiber Tracking and to implement it as a valid DBS preoperative planning technique.

Introduction

The use of deep brain stimulation (DBS) in parkinsonian tremor dates back to 1965 when Carl Wilhelm Sem-Jacobsen implanted depth electrodes to record and stimulate several thalamic targets in order to identify the best lesioning site in Parkinson's disease (PD). (Sem-Jacobsen, 1966; Sem-Jacobsen, 1965)

Besides PD various neuropsychiatric disorders as essential tremor (ET), dystonia and obsessive compulsive disorder warrant DBS .(Andrade et al., 2009; Miocinovic et al., 2013)

Despite the documented impact of DBS on numerous neuropsychiatric disorders (Andrade et al., 2009; Baldermann et al., 2016; Deuschl et al., 2006; Hardenacke et al., 2013; Milev et al., 2016; Morace et al., 2016; Parsons et al., 2006; Sako et al., 2014; Schuurman et al., 2000; Weaver et al., 2005), the optimal stimulation site to achieve tremor control is still debated. (Lim et al., 2010; Pollo et al., 2014) Increasing attention has been drawn to the dentatorubrothalamic tract (DRTT), a fine white matter fibers bundle connecting the cerebellum with the diencephalon.

Anatomy

The DRTT fibers initiate from the anterior medial part of nucleus dentatus (ND) (VOOGD, 2004) and ascend into the superior cerebellar peduncle (brachium conjunctivum). There some of its fibers produce a decussation over the mid-line moving from-right-to-left and vice versa within the mesencephalon (commissure of Wernekinck). Afterwards they run through- and anterior to- the nucleus ruber (NR). As the output fibers of the ND penetrate the NR in the midbrain, some terminate in its anterior parvocellular division.

From that point to the thalamus, the DRTT crosses the Zona Incerta from posterior to anterior when it goes from medial to lateral and from inferior to superior. It ends mainly in the ventral intermediate nucleus (Vim) and to a lesser extent, in the ventro-oralis posterior (Vop), the ventro-oralis anterior (Voa) which receives the main pallidal output, and the ventro-oralis medialis (V.o.m), according to Hassler's nomenclature.(Cagnan et al., 2014; Hassler, 1982; Morel et al., 1997) The Vim projects mainly to the primary motor cortex, to a lesser extent to the premotor cortex and to the supplementary motor area. The Vop projects to the primary motor cortex and the premotor cortex (Percheron et al., 1996) whereas the Voa projects mainly to the premotor cortex and to a lesser degree to the supplementary motor area and to the superior area of premotor cortex. (Blumenfeld, 2011; Khurana, 2014; Kulkarni, 2012; Sweet et al., 2014; Trepel, 2003)

Clinical impact

DRTT has come in the foreground by studies on PD (Sweet et al., 2014) and on ET.(Groppa et al., 2014; Plaha et al., 2004) The latter suggested that DBS in the posterior subthalamic area (PSA) might be related to the actual stimulation of the Dentatorubrothalamic tract (DRTT) in a deeper location where it crosses the PSA and the caudal zona incerta (cZi). Research exploring the optimal DBS target for PD has proposed the PSA (Carrillo-Ruiz et al., 2008), the cZi (Plaha, 2006; Plaha et al., 2008), the posterior zona incerta (Deuschl et al., 2006; Plaha, 2006; Pollo et al., 2007; Weise et al., 2013; Zonenshayn et al., 2004) and the prelemniscal radiation. (Carrillo-Ruiz et al., 2008) The last appears to relate to the rubrothalamic tract a division of DRTT. (Lemaire et al., 2011)

Irrespectively of the diagnostic indication for DBS, the DRTT was explored with diffusion tensor imaging (DTI) fiber tracking. (Anthofer et al., 2014; Coenen et al., 2011b, 2014; Gross et al., 2004; Hanson et al., 2012; Keane et al., 2012; Klein et al., 2012; Kumar et al., 1999; Perlmutter and Mink, 2006; Pollo et al., 2014; Schlaier et al., 2014; Sweet et al., 2014)

Acquisitions and fiber tracking

The fiber tracking (FT) technique relies on either DTI or DSI sequences of MRI. However when it comes to various fiber populations in intersecting axes per voxel, such as kissing, branching, crossing (eg. decussation of DRTT) of fibers (Basser and Jones, 2002; Coenen et al., 2011b; Descoteaux et al., 2009) DSI provides more accurate spatial resolution. (Abhinav et al., 2014; Beaulieu, 2002; Granziera et al., 2009) Moreover DSI acquires detailed information of the diffusion process, accounting for the tracts termination problem of white-to-grey matter transition(Hagmann et al., 2006; Wedeen et al., 2008, 2005). In terms of algorithm preference the deterministic algorithm for FT has proved instrumental in cranial operations and DBS procedures. (Coenen et al., 2011a, 2011b, 2014)

Given the lack of atlas-based coordinates of the DRTT the vast majority of DBS targeting has been relying on DTI FT since 2010 when the first promising preliminary clinical outcomes got published.(Coenen et al., 2011b; Fiechter et al., 2017; Plaha et al., 2004) We hypothesized that DRTT exists and explored the optimal way of characterizing it in a reproducible manner.

Materials And Methods

Patients

DSI sequence was performed on 10 adult human patients (5:5) suffering from PD who underwent preoperative investigation with brain MRI protocols prior to DBS at the University of Bern in Switzerland. (including anatomical MDEFT, MPRAGE with contrast and 3D T2 sequences as well). The patients' age ranged between 39 and 77 years (μ = 65.0). Ethics committee approval No 189/14; The University of Bern.

Included were the adults with tremor-dominant Parkinson disease from the DBS directory of Inselspital Bern from 2008 to 2014, who had a brain DSI- along with their standard T_2 sequence, for whom a DBS was indicated and conducted.

Excluded were the patients with incomplete preoperative imaging data and those with focal brain lesions, tumors or large bleeding areas which could affect the signal of MRI and alter the normal brain fiber tracts trajectory.

Protocol

The MRI examinations were performed at the Department of Diagnostic and Interventional Neuroradiology of the University Hospital of Bern with a 3-Tesla MRI system (Siemens Verio, Siemens Erlangen, Germany). All the acquired planes were parallel or orthogonal to the centres of the anterior and posterior commissures, according to the Talairach references for MRI. All DSI sequences of our sample were acquired using 32 channel RF and 128 diffusion encoding directions.

DSI

A q4half b6400 DSI sequence was used to the acquired diffusion images. The diffusion images were acquired using a DSI scheme. The DSI encoding used 515 gradient steps with 44 slices; bmax = 6400s mm^{-2} and yielded an image of Signal to Noise (SNR) in the cortex ≈ 100:1 at b = 0; TR: 8500 ms; TE: 154 ms; field of view: 212 mm; matrix: 96 × 96; slices: 44; slice thickness: 3.00 mm; voxel size: 2.2 × 2.2 × 3.0 mm; mean acquisition time: 18:42 minutes.

T_2

All images were acquired with sagittal orientation. The resulting data were reconstructed to an isotropic 1.0 mm^3 voxel size (3D). The T_2-weighted fast-spin-echo sequence was acquired with the following parameters: TR: 3200 ms; TE: 409 ms; field of view: 256 mm; matrix: 256 × 256; slices: 176; slices thickness: 1.0 mm; voxel size: 1.0 × 1.0 × 1.0 mm; mean acquisition time: 4:43 minutes.

Post-Processing of the Data

For each patient, the DSI acquisitions were fused with the corresponding T_2-weighted acquisitions by using the Matlab (MathWorks Inc, Natick, MA) package SPM (Wellcome Department of Imaging

Neuroscience; London, UK). The b0 DSI was used as reference image and the T_2 as source image. The final single data set images thickness of each fused T2-DSI slice was 2.2 mm as opposed to the initial thickness of each DSI slice of 3 mm.

Analysis

Fiber tracking analysis

The acquired data were analysed with Track Vis (*Ruopeng Wang, Van J. Wedeen, TrackVis.org, Martinos Centre for Biomedical Imaging, Massachusetts General Hospital*, www.trackvis.org*)*, a software tool for fiber tracking reconstruction, display and analysis that works with a deterministic algorithm(Wang et al., 2007).

As no systematic protocol for DRTT analysis using DSI exists up to now, the optimal values for the Angle- and Mask- thresholds were manually determined after calibration. After several trials the angle threshold was set at 60° and the mask threshold was set at 20.00 – 525.00. (Tables 1–2). The minimal fiber length threshold was set at 10 mm. The input files that were used for the DSI reconstruction were in DICOM (.dcm) and Nifti/Analyze (.nii) format. The reconstruction output files were in '.nii' format and the tractogramm output files in '.tract' format (Wang et al., 2007).

As a control check, the depiction of the decussation of the DRTT fibers at the level of the mesencephalon was attempted in all cases. In order to isolate the DRTT, three spherical regions of interest (ROI) were set according to the criteria of Kwon (Kwon et al., 2011). The first ROI was placed on the nucleus dentatus (ND), on an axial plane at a level where the anterior superior tip is first visible, contralateral to the Vim of interest. The second ROI was located on the superior cerebellar peduncle (SCP) contralateral to the Vim. Finally, a third ROI (diameter of two pixels, i.e. 4.4 mm) was set on the nucleus ruber (NR) at the axial plane of its maximal diameter, ipsilateral to the Vim of interest.

The original DSI images have been acquired parallel and orthogonal to the AC-PC (bicommisural) line, so that the three orthogonal planes of our anatomic images in TrackVIs keep in the AC-PC reference system.

In order to categorize our results based on the quantity of information they have been giving us, we suggested two criteria: 1) Firstly, the DRTT has to pass through all three ROIs: two contralateral ROIs to the thalamus of interest, namely the ND and SCP and one ipsilateral ROI to the thalamus of interest, namely the NR. 2) Secondly, in respect of the above prerequisites, the tract has to show a consistent crossing of its fibers at the level of the tegmentum mesencephali. The detection of this decussation has helped us distinguish the DRTT from the neighbouring fiber bundles.

If a case fulfilled both criteria it would fall into the first category, if it fulfilled only one it would fall into second and if it did not fulfil any criterion at all it would fall into the third category. More specifically if the identified DRTT would fulfil both criteria it would be regarded as completely successful. The cases that either had interrupted tracts, missing cerebellar or thalamic sections or didn't have a decussation were

regarded as incomplete. Finally the cases that had no adherence to the above mentioned criteria with random paths and inconsistent diffusion trajectories fell into the third category.

Results

The results of the identification of the DRTT with the proposed DSI approach were classified in the following three categories: 1) completely visible tract, 2) partially visible tract, and 3) non-visible tract. Complete bilateral tract identification was possible in 6 patients (60%), partially visible in 3 patients (30%), and non-visible in 1 patient (10%) (Figs. 1–3). The decussation took place in all of the cases at the level of the tegmentum mesencephali. (Table 1).

Course of DRTT

According to MRI anatomy

Nucleus dentatus - superior cerebellar peduncle

The course of our obtained tract and its relationships with the surrounding structures has been assessed on the DSI-T2 coregistered images. In all successfully identified cases, the tract stemmed from the antero-medial surface of ND and ascended forming the main body of superior cerebellar peduncle (SCP). The SCP is running antero-superiorly in bilateral symmetry reaching the brainstem and forming the lateral part of the roof of the fourth ventricle in its cranial half. Then the SCP courses just inferior to the inferior colliculus to reach the mesencephalon (Gallay et al., 2008; Hoch et al., 2016; Hong et al., 2010; Kramer et al., 2009)(Figs. 5.a-b).

Mesencephalon – Decussation

As the tract reaches the mesencephalon, it ascends from a postero-medial to an antero-lateral orientation up to the posterior part of the tectum mesencephali where the decussation takes place. Among the six patients with accurate visualization of the DRTT, the crossing of fibers happened either exactly at the level of the maximal axial diameter of the NR, or 3, 6 or 9 mm inferior to that plane, with a sample prevalence of 1: 1: 2: 2, respectively in 17% ,17%, 33% and 33% of the group. Right after the decussation the DRTT climbs on a distance of 3 to 6 mm just posterior to SN following the same antero-superior direction.

Red Nucleus

From there, the DRTT moves in the direction of NR and passes through its antero-lateral and inferior surface. Then, the tract ascends from a postero-inferior to antero-superior direction with a ~ 60° angle in the sagittal plane (Fig. 6.a) and from a medio-inferior to latero-superior direction with a ~ 45° angle in the coronal plane (Fig. 6.b). According to the Latin literature, the tract is named “fasciculus cerebellothalamicus” on its route from the NR to its entrance in the thalamus (Gallay et al., 2008; Morel, 2007) .

Thalamus

The tract enters the thalamus in the inferior and posterior part of its lateral half. By entering the thalamus the tract changes direction, from 60° to an approximate 80° angle in the sagittal plane and from 45° to 60° angle in the coronal plane.

The basic source of reference has been the anatomical atlas of Morel(Morel, 2007). According to it, the trajectory of the tract is: 1) toward the posterior part of the “ventral medial” (VM) nucleus, 2) the “ventral lateral” posterior nucleus (VLp), 3) possibly the VLa and sometimes 4) the intralaminar nuclei.

As long as the tract moved through thalamus it kept the 60° angle in the coronal plane. After exiting thalamus the coronal plane angle switched again to 45° (Figs. 7.a-b). The intrathalamic endpoint of the tract is in keeping with the V.im/Vop nuclei. However, due to the resolution limitation of actual imaging techniques in the representation of thalamic subterritories as well as the co-registration of the anatomic sequences with the big voxel-based DSI sequences and consecutive low images resolution, the exact thalamic endpoint of DRTT could not be identified with high precision. Structures like the spinothalamic tract, lemniscus medialis and the prelemniscal radiation couldn’t likewise be precisely identified.

Cortex

After leaving the thalamus, the DRTT spreads its fibers in the Corona Radiata to finally reach the motor and premotor cortex, identified in T2 sequences according to Yousry et al (Percheron et al., 1996; Yousry et al., 1997) (Fig. 8).

According to AC-PC plane

Axial plane

In the axial plane, at the level where NR acquires its maximum diameter, the tract runs precisely between the antero-lateral surface of the NR and the postero-medial part of the STh (Fig. 9). According to the Morel Atlas, our main reference source, the bulk of the DRTT is posterior and lateral to the pallidothalamic tract, and they come close together at some levels but still separated (Morel, 2007).

In our study the DRTT could be observed on the axial views of all the 6 successfully depicted cases. (Figs. 9–10).

Coronal plane

The tract ascended in a 45° angle from mesencephalon into the direction of thalamus. It courses between NR and STh/ SN (Fig. 11). Similar results were obtained in all of our cases with successful visualisation of the tract.

Sagittal plane

During its whole course from mesencephalon to thalamus the DRTT kept ascending posteriorly and partially in parallel to STh and SN (Fig. 13).

Discussion

Based on results

Our study is a first attempt to depict specifically the DRTT in living patient suffering from PD using a similar approach. We were able to identify and depict the whole DRTT using high angular DSI performed at 3T. Our results were consistent with the anatomical course of the tract (Gallay et al., 2008; Percheron et al., 1996) .

The decussation could be observed in six of the ten subjects from 0 to 9 mm inferior to the level of the maximal diameter of the NR in the axial plane. This observed variability of the fibers decussation has not been previously reported and whether it represents a real inter-individual variability or results from an erroneous reconstruction of the crossing fibers with the chosen algorithm is not known. One must keep in mind that the demonstrated tracts are representations of water molecules diffusion along the axons rather than radiological depiction of a real anatomic structure (Sarubbo et al., 2013; Schmahmann et al., 2007). However, the fact that the DRTT crossed the midline at the same level on both hemispheres for each successful case supports the hypothesis of a consistent representation of the decussation.

Although the DRTT has been successfully represented in its entirety in 60% cases, in 40% of the sample, the tract could be either only partially depicted, or not identified at all. These results could be explained through technical limitations of the used approach (namely insufficient number of read-out directions, low strength of MRI field or inadequate voxel size during images acquisition, suboptimal ROI placement and faulty reconstruction with the chosen algorithm during fiber tracking process) (Holl et al., 2011; Martino et al., 2013; Middlebrooks et al., 2015). The specific population used for this study may also explain this observation, as diffuse gray and white matter brain atrophy has been associated with Parkinson’s disease, consequently decreasing the strength of diffusion along the tract. Moreover, even if quantitative/qualitative changes along the DRTT were beyond the scope of this study, this abnormality could actually characterize a biomarker of tremor in this population, as it was already suggested in DTI-based studies that fractional anisotropy (FA) could reflect changes in the fiber organisation with a reduction in cases of axonal degeneration (Martino et al., 2013; Middlebrooks et al., 2015). Longitudinal studies could be a valuable tool to assess possible quantitative and qualitative changes in the course of PD.

In one case, the DRTT could be depicted with only one ROI directly centered on the NR (radius of two pixels, corresponding to 4.4 mm), with a course very similar to the tracts obtained with the above-described three ROI approach, in terms of location and orientation of the fiber bundles. The absence of other fiber tracts (e.g. rubrospinal tract running toward the spinal cord or corticospinal fibers running in the cerebral peduncle nearby the ROI) was notable. In that case the number of fibers were minimal.

DRTT as DBS target

In regards to the DRTT appropriateness Schlaier et al (Anthofer et al., 2014; Schlaier et al., 2014) could not find a clear correlation between tremor reduction and the distance between the stimulating electrode and the DRTT. They suggested that the precise identification of the DRTT on DTI may be a limiting factor and proposed that DTI sequences with a higher number of read-out directions, probabilistic fiber tracking and 3 T MRI scanners may lead to different results in the depiction of the chosen fiber tract and may provide a better correlation with stimulation effects. Even if DSI techniques have shown superiority on DTI in identifying fiber crossing, complex structures (e.g. in the centrum semiovale, the pontocerebellar fibers in the basis pontis) and fibers entering into gray matter of cortical regions (Wedeen et al., 2008), further studies are mandatory to investigate (1) the safety and efficacy of DSI in accurately depicting the DRTT for DBS as well as (2) correlate the position of the identified DRTT with the stimulation site and the clinical outcomes in larger cohorts of patients. Finally integration of softwares able to process DSI data, in the usual stereotactic planning platforms is needed to investigate the reliability and accuracy of DSI to target the DRTT in the clinical practice.

Limitations

Concerning the bad delineation a possible explanation may be the difficulty of the algorithm to analyse white matter tracts at the level of the pons or even more posterior to it. The algorithm used seems to be unable to make definitive distinctions between the fine thin DRTT from the adjacent structures like the medial lemniscus or the spinothalamic tract and we should always take into account the possibility of biased results (Holl et al., 2011).

Beyond the previously mentioned technical limitations of the sequence, the small sample of patients precludes the generalization of our results to other subjects suffering from PD. Moreover, we were not able to correlate our findings with postmortem verification of the DRTT in these patients. There are reports in the recent literature of successful validation of the depicted white matter tracts with DSI algorithm by means of fiber dissection in human postmortem brain. (Schmahmann et al., 2007) The group of Fernandez-Miranda and al. were able to depict fibers originating from the ND, terminating in the contralateral NR and thalamus, after their decussation at the level of the lower midbrain, with a whole-brain DSI fiber tracking procedure and an orientation distribution function–streamlined region of interest– based approach.(Fernandez-Miranda et al., 2012) This might provide solid basis for the further development validation approaches to corroborate the DSI based DRTT representation with the classical anatomohistological data (Holl et al., 2011; Martino et al., 2013; Middlebrooks et al., 2015; Sarubbo et al., 2013; Schmahmann et al., 2007) .

Finally, The data output format after processing the images with Trackvis (i.e. Nifti/Analyze (.nii)), may raise concerns about the technical feasibility of their integration in the current planning platforms for DBS, in order to perform the preoperative targeting and to visualize the stimulation location in relation to the depicted DRTT.

Conclusions

In this study, we implemented an innovative DSI tractography approach to depict *in vivo* the DRTT tract in human patients suffering from Parkinson's disease. The delineated DRTT showed a high consistency with the existing anatomical data. Therefore, DSI algorithm might be used in the future to precisely identify and target the DRTT in DBS for tremor and in order to reliably demonstrate the anatomic relations of the stimulating site with the targeted tract in postoperative MR imaging. Further research is needed to optimize the image resolution, the tractography algorithms and to improve the reliability of DSI.

The accuracy and reliability of DSI in precisely identifying the actual anatomical location of the DRTT, especially in the subthalamic region used for DBS targeting, remains unclear, DSI has shown potential advantages to overcome the limitations of DTI in identifying fiber tracts precisely. No systematic analysis of the DRTT has been performed so far using this technique. This is relevant for precise targeting and electrode placement when considering DBS for tremor.

Abbreviations

ADC	apparent diffusion coefficient
DBS	deep brain stimulation
DRTT	dentatorubrothalamic tract
DSI	diffusion spectrum imaging
DTI	diffusion tensor imaging
DWI	diffusion weighted imaging
ET	essential tremor
GPi	globus pallidus internus
MRI	magnetic resonance imaging
ND	nucleus dentatus
NMV	net magnetization vector
NR	nucleus ruber
PD	Parkinson's disease
PSA	Posterior subthalamic area

SN	Substantia nigra
SPCT	subthalamo-ponto-cerebellar tract
STh	nucleus subthalamicus
Vim	ventral intermediate nucleus (also known as the VLp)
VLa	nucleus ventralis lateralis anterior
VLp	nucleus ventralis lateralis posterior
Voa	nucleus ventro-oralis anterior
Vop	nucleus ventro-oralis posterior

Declarations

Funding: No funding has been applied on this project .

Conflicts of interest/Competing interests: The author confirms that there have been no conflicts of interest .

Ethics approval: The project has been approved by the Ethics committee of the University hospital of Bern, Switzerland. (ref.nr. 189-14 version 3)

Consent to participate: every individual has consented to participate

Consent for publication: every individual has consented for publication

Availability of data and material: data transparency principles have applied

Code availability: all data have been anonymised, coded, secured and stored in the database of University Hospital of Bern

Authors' contributions: the main author and all co-authors have contributed in the realization of this project

Data availability

1. The datasets generated during and/or analysed during the current study are available in the University Hospital of Bern, Switzerland database repository.
2. The datasets generated during and/or analysed during the current study are available from the corresponding author on reasonable request.

3. All data generated or analysed during this study are included in this published article [and its supplementary information files].
4. The datasets generated during and/or analysed during the current study are not publicly available due to Rights of patient confidentiality [but are available from the corresponding author on reasonable request.].
5. Data sharing not applicable to this article as no datasets were generated or analysed during the current study.
6. The data that support the findings of this study are available from University Hospital of Bern database but restrictions apply to the availability of these data, which were used under licence for the current study, and so are not publicly available. Data are however available from the authors upon reasonable request and with permission of University Hospital of Bern.

References

Abhinav, K., Yeh, F.C., Pathak, S., Suski, V., Lacomis, D., Friedlander, R.M., Fernandez-Miranda, J.C., 2014. Advanced diffusion MRI fiber tracking in neurosurgical and neurodegenerative disorders and neuroanatomical studies: A review. Biochim. Biophys. Acta - Mol. Basis Dis. 1842, 2286–2297. https://doi.org/10.1016/j.bbadis.2014.08.002

Andrade, P., Carrillo-Ruiz, J.D., Jiménez, F., 2009. A systematic review of the efficacy of globus pallidus stimulation in the treatment of Parkinson's disease. J. Clin. Neurosci. 16, 877–881. https://doi.org/10.1016/j.jocn.2008.11.006

Anthofer, J., Steib, K., Fellner, C., Lange, M., Brawanski, A., Schlaier, J., 2014. The variability of atlas-based targets in relation to surrounding major fibre tracts in thalamic deep brain stimulation. Acta Neurochir. (Wien). 156, 1497–504; discussion 1504. https://doi.org/10.1007/s00701-014-2103-z

Baldermann, J.C., Schüller, T., Huys, D., Becker, I., Timmermann, L., Jessen, F., Visser-Vandewalle, V., Kuhn, J., 2016. Deep Brain Stimulation for Tourette-Syndrome: A Systematic Review and Meta-Analysis. Brain Stimul. 9, 296–304. https://doi.org/10.1016/j.brs.2015.11.005

Basser, P.J., Jones, D.K., 2002. Diffusion-tensor MRI: theory, experimental design and data analysis–a technical review. NMR Biomed 15, 456–467. https://doi.org/10.1002nbm.783

Beaulieu, C., 2002. The basis of anisotropic water diffusion in the nervous system - a technical review. NMR Biomed. 15, 435–55. https://doi.org/10.1002/nbm.782

Blumenfeld, H., 2011. Neuroanatomy Through Clinical Cases, 2nd ed. Sinauer Associates, Inc.

Cagnan, H., Little, S., Foltynie, T., Limousin, P., Zrinzo, L., Hariz, M., Cheeran, B., Fitzgerald, J., Green, A.L., Aziz, T., Brown, P., 2014. The nature of tremor circuits in parkinsonian and essential tremor. Brain 137, 3223–3234. https://doi.org/10.1093/brain/awu250

Carrillo-Ruiz, J.D., Velasco, F., Jimènez, F., Castro, G., Velasco, A.L., Hernández, J.A., Ceballos, J., Velasco, M., 2008. Bilateral electrical stimulation of prelemniscal radiations in the treatment of advanced Parkinson's disease. Neurosurgery 62, 347–57; discussion 357-9. https://doi.org/10.1227/01.neu.0000316001.03765.e8

Coenen, V. a., Allert, N., Mädler, B., 2011a. A role of diffusion tensor imaging fiber tracking in deep brain stimulation surgery: DBS of the dentato-rubro-thalamic tract (drt) for the treatment of therapy-refractory tremor. Acta Neurochir. (Wien). 153, 1579–1585. https://doi.org/10.1007/s00701-011-1036-z

Coenen, V. a., Mädler, B., Schiffbauer, H., Urbach, H., Allert, N., 2011b. Individual fiber anatomy of the subthalamic region revealed with diffusion tensor imaging: A concept to identify the deep brain stimulation target for tremor suppression. Neurosurgery 68, 1069–1076. https://doi.org/10.1227/NEU.0b013e31820a1a20

Coenen, V.A., Allert, N., Paus, S., Kronenbürger, M., Urbach, H., Mädler, B., 2014. Modulation of the Cerebello-Thalamo-Cortical Network in Thalamic Deep Brain Stimulation for Tremor. Neurosurgery 75, 657–670. https://doi.org/10.1227/NEU.0000000000000540

Descoteaux, M., Deriche, R., Knösche, T.R., Anwander, A., 2009. Deterministic and Probabilistic Tractography Based on Complex Fibre Orientation Distributions 28, 269–286.

Deuschl, G., Schade-Brittinger, C., Krack, P., Volkmann, J., Schäfer, H., Bötzel, K., Daniels, C., Deutschländer, A., Dillmann, U., Eisner, W., Gruber, D., Hamel, W., Herzog, J., Hilker, R., Klebe, S., Kloss, M., Koy, J., Krause, M., Kupsch, A., Lorenz, D., Lorenzl, S., Mehdorn, H.M., Moringlane, J.R., Oertel, W., Pinsker, M.O., Reichmann, H., Reuss, A., Schneider, G.-H., Schnitzler, A., Steude, U., Sturm, V., Timmermann, L., Tronnier, V., Trottenberg, T., Wojtecki, L., Wolf, E., Poewe, W., Voges, J., German Parkinson Study Group, Neurostimulation Section, 2006. A randomized trial of deep-brain stimulation for Parkinson's disease. N. Engl. J. Med. 355, 896–908. https://doi.org/10.1056/NEJMoa060281

Fernandez-Miranda, J.C., Pathak, S., Engh, J., Jarbo, K., Verstynen, T., Yeh, F.C., Wang, Y., Mintz, A., Boada, F., Schneider, W., Friedlander, R., 2012. High-definition fiber tractography of the human brain: Neuroanatomical validation and neurosurgical applications. Neurosurgery 71, 430–453. https://doi.org/10.1227/NEU.0b013e3182592faa

Fiechter, M., Nowacki, A., Oertel, M.F., Fichtner, J., Debove, I., Lachenmayer, M.L., Wiest, R., Bassetti, C.L., Raabe, A., Kaelin-Lang, A., Schüpbach, M.W., Pollo, C., 2017. Deep Brain Stimulation for Tremor: Is There a Common Structure? Stereotact. Funct. Neurosurg. 95, 243–250. https://doi.org/10.1159/000478270

Gallay, M.N., Jeanmonod, D., Liu, J., Morel, A., 2008. Human pallidothalamic and cerebellothalamic tracts: Anatomical basis for functional stereotactic neurosurgery. Brain Struct. Funct. 212, 443–463. https://doi.org/10.1007/s00429-007-0170-0

Granziera, C., Schmahmann, J.D., Hadjikhani, N., Meyer, H., Meuli, R., Wedeen, V., Krueger, G., 2009. Diffusion spectrum imaging shows the structural basis of functional cerebellar circuits in the human cerebellum in vivo. PLoS One 4, 1–6. https://doi.org/10.1371/journal.pone.0005101

Groppa, S., Herzog, J., Falk, D., Riedel, C., Deuschl, G., Volkmann, J., 2014. Physiological and anatomical decomposition of subthalamic neurostimulation effects in essential tremor. Brain 137, 109–21. https://doi.org/10.1093/brain/awt304

Gross, R.E., Jones, E.G., Dostrovsky, J.O., Bergeron, C., Lang, A.E., Lozano, A.M., 2004. Histological analysis of the location of effective thalamic stimulation for tremor. Case report. J. Neurosurg. 100, 547–52. https://doi.org/10.3171/jns.2004.100.3.0547

Hagmann, P., Jonasson, L., Maeder, P., Thiran, J.-P., Wedeen, V.J., Meuli, R., 2006. Understanding Diffusion MR Imaging Techniques: From Scalar Diffusion-weighted Imaging to Diffusion Tensor Imaging and Beyond. RadioGraphics 26, S205–S223. https://doi.org/10.1148/rg.26si065510

Hanson, T.L., Fuller, A.M., Lebedev, M.A., Turner, D.A., Nicolelis, M.A.L., 2012. Subcortical Neuronal Ensembles: An Analysis of Motor Task Association, Tremor, Oscillations, and Synchrony in Human Patients. J. Neurosci. 32, 8620–8632. https://doi.org/10.1523/JNEUROSCI.0750-12.2012

Hardenacke, K., Shubina, E., Bührle, C.P., Zapf, A., Lenartz, D., Klosterkötter, J., Visser-Vandewalle, V., Kuhn, J., 2013. Deep Brain Stimulation as a Tool for Improving Cognitive Functioning in Alzheimer's Dementia: A Systematic Review. Front. Psychiatry 4, 159. https://doi.org/10.3389/fpsyt.2013.00159

Hassler, R., 1982. Architectonic organization of the thalamic nuclei in: Schaltenbrand G, Walker AE (eds) Stereotaxy of the human brain. Anatomical, physiological and clinical applications. Thieme, Stuttgart.

Hoch, M.J., Chung, S., Ben-Eliezer, N., Bruno, M.T., Fatterpekar, G.M., Shepherd, T.M., 2016. New clinically feasible 3T MRI protocol to discriminate internal brain stem anatomy. Am. J. Neuroradiol. 37, 1058–1065. https://doi.org/10.3174/ajnr.A4685

Holl, N., Noblet, V., Rodrigo, S., Dietemann, J.L., Mekhbi, M. Ben, Kehrli, P., Wolfram-Gabel, R., Braun, M., Kremer, S., 2011. Temporal lobe association fiber tractography as compared to histology and dissection. Surg. Radiol. Anat. 33, 713–22. https://doi.org/10.1007/s00276-011-0816-8

Hong, J.H., Son, S.M., Jang, S.H., 2010. Identification of spinothalamic tract and its related thalamocortical fibers in human brain. Neurosci. Lett. 468, 102–105. https://doi.org/10.1016/j.neulet.2009.10.075

Keane, M., Deyo, S., Abosch, A., Bajwa, J.A., Johnson, M.D., 2012. Improved spatial targeting with directionally segmented deep brain stimulation leads for treating essential tremor. J. Neural Eng. 9, 046005. https://doi.org/10.1088/1741-2560/9/4/046005

Khurana, I., 2014. Textbook Of Medical Physiology, 2nd ed. Elsevier India Pvt.ltd.

Klein, J.C., Barbe, M.T., Seifried, C., Baudrexel, S., Runge, M., Maarouf, M., Gasser, T., Hattingen, E., Liebig, T., Deichmann, R., Timmermann, L., Weise, L., Hilker, R., 2012. The tremor network targeted by successful VIM deep brain stimulation in humans. Neurology 78, 787–795. https://doi.org/10.1212/WNL.0b013e318249f702

Kramer, L.A., Butler, I.J., Kamali, A., Kramer, L.A., Butler, I.J., Hasan, K.M., 2009. Diffusion tensor tractography of the somatosensory system in the human brainstem : initial findings using high isotropic spatial resolution at 3 . 0 T. Eur. Radiol. 17, 1480–1488. https://doi.org/10.1007/s00330-009-1305-x

Kulkarni, N., 2012. Clinical Anatomy (A Problem Solving Approach). Jaypee Brothers Medical Publishers (P) Ltd. https://doi.org/10.5005/jp/books/11489

Kumar, K., Kelly, M., Toth, C., 1999. Deep brain stimulation of the ventral intermediate nucleus of the thalamus for control of tremors in Parkinson's disease and essential tremor. Stereotact. Funct. Neurosurg. 72, 47–61. https://doi.org/29671

Kwon, H.G., Hong, J.H., Hong, C.P., Lee, D.H., Ahn, S.H., Jang, S.H., 2011. Dentatorubrothalamic tract in human brain: Diffusion tensor tractography study. Neuroradiology 53, 787–791. https://doi.org/10.1007/s00234-011-0878-7

Lemaire, J.-J., Cosnard, G., Sakka, L., Nuti, C., Gradkowski, W., Mori, S., Hermoye, L., 2011. White matter anatomy of the human deep brain revisited with high resolution DTI fibre tracking. Neurochirurgie 57, 52–67. https://doi.org/10.1016/j.neuchi.2011.04.001

Lim, S.Y., Hodaie, M., Fallis, M., Poon, Y.Y., Mazzella, F., Moro, E., 2010. Gamma knife thalamotomy for disabling tremor: a blinded evaluation. Arch Neurol 67, 584–588. https://doi.org/10.1001/archneurol.2010.69

Martino, J., Da Silva-Freitas, R., Caballero, H., Marco De Lucas, E., Garc??a-Porrero, J.A., V??zquez-Barquero, A., 2013. Fiber dissection and diffusion tensor imaging tractography study of the temporoparietal fiber intersection area. Neurosurgery 72. https://doi.org/10.1227/NEU.0b013e318274294b

Middlebrooks, E.H., Yagmurlu, K., Bennett, J.A., Bidari, S., 2015. Normal relationship of the cervicomedullary junction with the obex and olivary bodies: a comparison of cadaveric dissection and in vivo diffusion tensor imaging. Surg. Radiol. Anat. 37, 493–497. https://doi.org/10.1007/s00276-014-1387-2

Milev, R. V., Giacobbe, P., Kennedy, S.H., Blumberger, D.M., Daskalakis, Z.J., Downar, J., Modirrousta, M., Patry, S., Vila-Rodriguez, F., Lam, R.W., MacQueen, G.M., Parikh, S. V., Ravindran, A. V., CANMAT Depression Work Group, 2016. Canadian Network for Mood and Anxiety Treatments (CANMAT) 2016 Clinical Guidelines for the Management of Adults with Major Depressive Disorder. Can. J. Psychiatry 61, 561–575. https://doi.org/10.1177/0706743716660033

Miocinovic, S., Somayajula, S., Chitnis, S., Vitek, J.L., 2013. History, applications, and mechanisms of deep brain stimulation. JAMA Neurol. 70, 163–71. https://doi.org/10.1001/2013.jamaneurol.45

Morace, R., DI Gennaro, G., Quarato, P., D'Aniello, A., Amascia, A., Grammaldo, L., DE Risi, M., Sparano, A., DE Angelis, M., DI Cola, F., Solari, D., Esposito, V., 2016. Deep brain stimulation for intractabile epilepsy. J. Neurosurg. Sci. 60, 189–98.

Morel, A., 2007. Stereotactic atlas of the human thalamus and basal ganglia. Informa Healthcare, New York, 1st ed. Informa Healthcare USA, Inc.

Morel, A., Magnin, M., Jeanmonod, D., 1997. Multiarchitectonic and stereotactic atlas of the human thalamus. J. Comp. Neurol. 387, 588–630.

Parsons, T.D., Rogers, S.A., Braaten, A.J., Woods, S.P., Tröster, A.I., 2006. Cognitive sequelae of subthalamic nucleus deep brain stimulation in Parkinson's disease: a meta-analysis. Lancet Neurol. 5, 578–588. https://doi.org/10.1016/S1474-4422(06)70475-6

Percheron, G., François, C., Talbi, B., Yelnik, J., Fénelon, G., 1996. The primate motor thalamus. Brain Res. Brain Res. Rev. 22, 93–181.

Perlmutter, J.S., Mink, J.W., 2006. Deep brain stimulation. Annu. Rev. Neurosci. 29, 229–57. https://doi.org/10.1146/annurev.neuro.29.051605.112824

Plaha, P., 2006. Stimulation of the caudal zona incerta is superior to stimulation of the subthalamic nucleus in improving contralateral parkinsonism. Brain 129, 1732–1747. https://doi.org/10.1093/brain/awl127

Plaha, P., Khan, S., Gill, S.S., 2008. Bilateral stimulation of the caudal zona incerta nucleus for tremor control. J. Neurol. Neurosurg. Psychiatry 79, 504–513. https://doi.org/10.1136/jnnp.2006.112334

Plaha, P., Patel, N.K., Gill, S.S., 2004. Stimulation of the subthalamic region for essential tremor. J. Neurosurg. 101, 48–54. https://doi.org/10.3171/jns.2004.101.1.0048

Pollo, C., Kaelin-Lang, A., Oertel, M.F., Stieglitz, L., Taub, E., Fuhr, P., Lozano, A.M., Raabe, A., Schüpbach, M., 2014. Directional deep brain stimulation: An intraoperative double-blind pilot study. Brain 137, 2015–2026. https://doi.org/10.1093/brain/awu102

Pollo, C., Vingerhoets, F., Pralong, E., Ghika, J., Maeder, P., Meuli, R., Thiran, J.-P., Villemure, J.-G., 2007. Localization of electrodes in the subthalamic nucleus on magnetic resonance imaging. J. Neurosurg. 106, 36–44. https://doi.org/10.3171/jns.2007.106.1.36

Sako, W., Miyazaki, Y., Izumi, Y., Kaji, R., 2014. Which target is best for patients with Parkinson's disease? A meta-analysis of pallidal and subthalamic stimulation. J. Neurol. Neurosurg. Psychiatry 85, 982–986. https://doi.org/10.1136/jnnp-2013-306090

Sarubbo, S., De Benedictis, A., Maldonado, I.L., Basso, G., Duffau, H., 2013. Frontal terminations for the inferior fronto-occipital fascicle: Anatomical dissection, DTI study and functional considerations on a multi-component bundle. Brain Struct. Funct. 218, 21–37. https://doi.org/10.1007/s00429-011-0372-3

Schlaier, J., Anthofer, J., Steib, K., Fellner, C., Rothenfusser, E., Brawanski, A., Lange, M., 2014. Deep Brain Stimulation for Essential Tremor: Targeting the Dentato-Rubro-Thalamic Tract? Neuromodulation Technol. Neural Interface 2014, n/a-n/a. https://doi.org/10.1111/ner.12238

Schmahmann, J.D., Pandya, D.N., Wang, R., Dai, G., D'Arceuil, H.E., de Crespigny, A.J., Wedeen, V.J., D'Arceuil, H.E., de Crespigny, A.J., Wedeen, V.J., 2007. Association fibre pathways of the brain: Parallel observations from diffusion spectrum imaging and autoradiography. Brain 130, 630–653. https://doi.org/10.1093/brain/awl359

Schuurman, P.R., Bosch, D.A., Bossuyt, P.M., Bonsel, G.J., van Someren, E.J., de Bie, R.M., Merkus, M.P., Speelman, J.D., 2000. A comparison of continuous thalamic stimulation and thalamotomy for suppression of severe tremor. N. Engl. J. Med. 342, 461–8. https://doi.org/10.1056/NEJM200002173420703

Sem-Jacobsen, C.W., 1966. Depth-electrographic observations related to Parkinson's disease. Recording and electrical stimulation in the area around the third ventricle. J. Neurosurg. 24, Suppl:388-402.

Sem-Jacobsen, C.W., 1965. DEPTH ELECTROGRAPHIC STIMULATION AND TREATMENT OF PATIENTS WITH PARKINSON'S DISEASE INCLUDING NEUROSURGICAL TECHNIQUE. Acta Neurol. Scand. 41, 365–376. https://doi.org/10.1111/j.1600-0404.1965.tb01899.x

Sweet, J. a, Walter, B.L., Gunalan, K., Chaturvedi, A., McIntyre, C.C., Miller, J.P., 2014. Fiber tractography of the axonal pathways linking the basal ganglia and cerebellum in Parkinson disease: implications for targeting in deep brain stimulation. J. Neurosurg. 120, 988–96. https://doi.org/10.3171/2013.12.JNS131537

Trepel, M., 2003. Neuroanatomie, Struktur und Funktion, 2nd ed. Urban & Fischer Verlag/Elsevier GmbH, Munich.

VOOGD, J., 2004. Cerebellum and Precerebellar Nuclei, in: The Human Nervous System. Elsevier, pp. 321–392. https://doi.org/10.1016/B978-012547626-3/50012-0

Wang, R., Benner, T., Sorensen, a G., Wedeen, V.J., 2007. Diffusion Toolkit : A Software Package for Diffusion Imaging Data Processing and Tractography. Proc. Intl. Soc. Mag. Reson. Med. 15, 3720.

Weaver, F., Follett, K., Hur, K., Ippolito, D., Stern, M., 2005. Deep brain stimulation in Parkinson disease: a metaanalysis of patient outcomes. J. Neurosurg. 103, 956–967. https://doi.org/10.3171/jns.2005.103.6.0956

Wedeen, V.J., Hagmann, P., Tseng, W.Y.I., Reese, T.G., Weisskoff, R.M., 2005. Mapping complex tissue architecture with diffusion spectrum magnetic resonance imaging. Magn. Reson. Med. 54, 1377–1386. https://doi.org/10.1002/mrm.20642

Wedeen, V.J., Wang, R.P., Schmahmann, J.D., Benner, T., Tseng, W.Y.I., Dai, G., Pandya, D.N., Hagmann, P., D'Arceuil, H., de Crespigny, a. J., 2008. Diffusion spectrum magnetic resonance imaging (DSI) tractography of crossing fibers. Neuroimage 41, 1267–1277. https://doi.org/10.1016/j.neuroimage.2008.03.036

Weise, L.M., Seifried, C., Eibach, S., Gasser, T., Roeper, J., Seifert, V., Hilker, R., 2013. Correlation of active contact positions with the electrophysiological and anatomical subdivisions of the subthalamic nucleus in deep brain stimulation. Stereotact. Funct. Neurosurg. 91, 298–305. https://doi.org/10.1159/000345259

Yousry, T. a., Schmid, U.D., Alkadhi, H., Schmidt, D., Peraud, a., Buettner, a., Winkler, P., 1997. Localization of the motor hand area to a knob on the precentral gyrus. A new landmark. Brain 120, 141–157. https://doi.org/10.1093/brain/120.1.141

Zonenshayn, M., Sterio, D., Kelly, P.J., Rezai, A.R., Beric, A., 2004. Location of the active contact within the subthalamic nucleus (STN) in the treatment of idiopathic Parkinson's disease. Surg. Neurol. 62, 216–25; discussion 225-6. https://doi.org/10.1016/j.surneu.2003.09.039

Tables

Table 1

Angle threshold attempts from 20° to 90°. Standard Mask: 20.84 – 525.01. All the measurements have been made on the b0 DSI images. Symbols interpretation: - : no Tract. + : incomplete tract. ++ : successful tract. Coordinates expressed in pixel units of XYZ axes. Dec: stands for the superior cerebellar peduncle decussation projected on the Z axis.

Patient	20°	35°	45°	60°	70°	80°	90°	NR left	NR right	Decussation	successful DRTT
1	-	-	++	++	++	++	++	(51 ,52, 15)	(45, 52, 15)	Decussation: 13	+
2	-	-	+	+	+	+	+	(52, 51, 18)	(47, 51, 18)	No Dec.	-
3	-	-	+	+	+	+	+	(50, 51, 17)	(46, 51, 17)	No Dec.	-
4	-	-	-	+	+	+	+	(52, 52, 18)	(47 ,51, 18)	No Dec.	-
5	-	-	+	++	++	++	++	(51, 47, 17)	(46, 47, 17)	Dec: 16	+
6	-	-	-	++	++	++	++	(51, 52, 17)	(46, 52, 17)	Dec: 17	+
7	-	-	-	++	++	++	++	(52, 53, 18)	(47, 53, 18)	Dec: 15	+
8	-	-	-	++	++	++	++	(53, 51, 17)	(47, 50, 17)	Dec: 14	+
9	-	-	-	-	-	-	-	(53, 51, 15)	(47, 51, 15)	No Dec.	-
10	-	-	-	++	++	++	++	(51, 52, 20)	(46, 52, 20)	Dec: 18	+

Decussation: 6; DRTT: 6.

Table 2

Mask threshold attempts from 0 to 525,0. Standard Angle: 60°. All the measurements have been made on the b0 DSI images. Symbols interpretation: - : no Tract. + : incomplete tract. ++ : successful tract.

Patient	44-525	44-288	288-525	166-410	44-1025	0-525	10-525	20-525	30-525
1	-	-	-	-	-	+	+	++	-
2	-	-	-	-	-	+	+	+	-
3	-	-	-	-	-	+	+	+	-
4	-	-	-	-	-	+	+	+	-
5	-	-	-	-	-	+	+	++	-
6	-	-	-	-	-	+	+	++	-
7	-	-	-	-	-	+	+	++	-
8	-	-	-	-	-	+	+	++	-
9	-	-	-	-	-	+	+	+	-
10	-	-	-	-	-	+	+	++	-

Figures

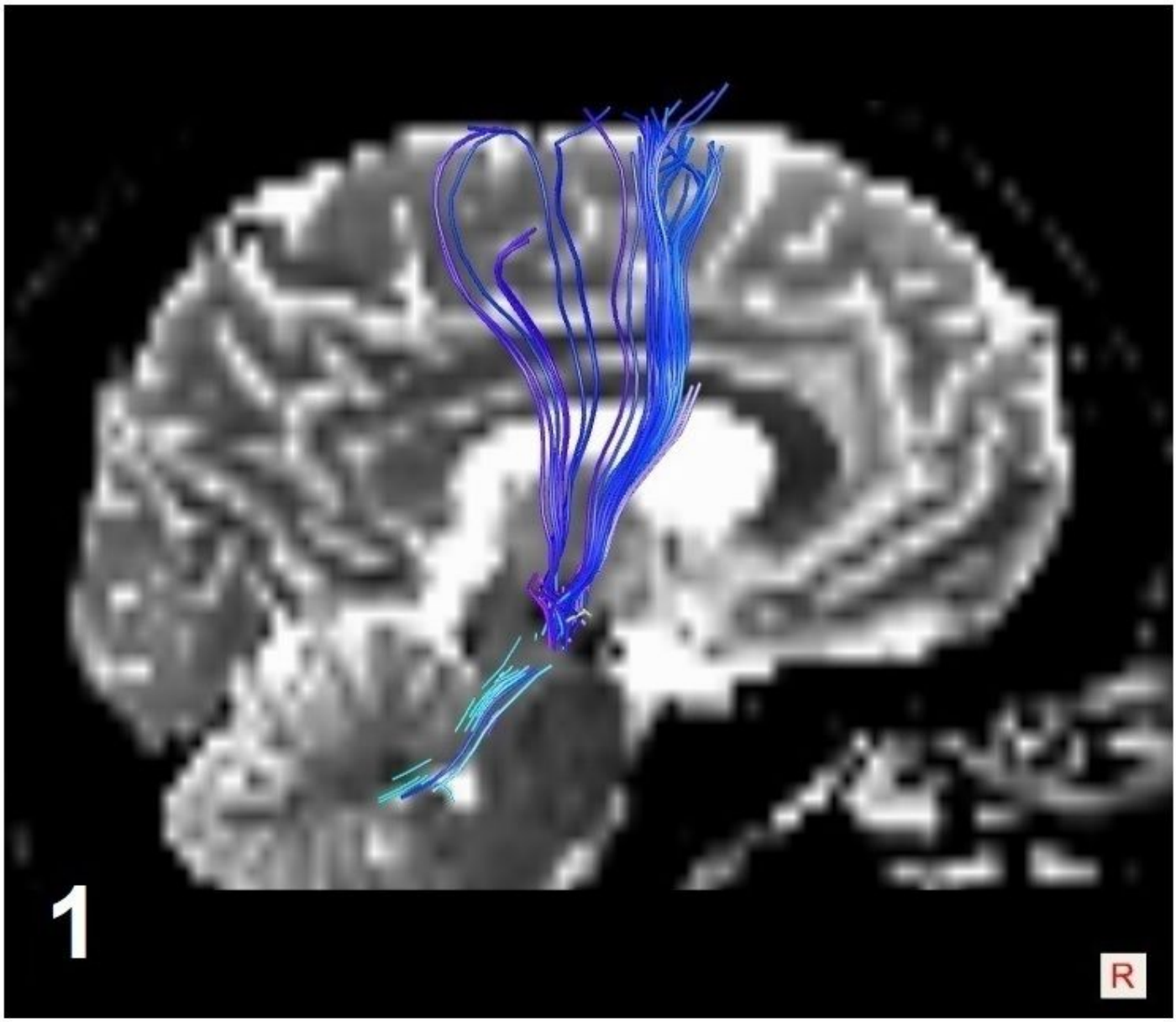

Figure 1

DSI-T2 fusion. Sagittal views.DRTT depicted as a completely visible tract from nucleus dentatus to frontal lobe.

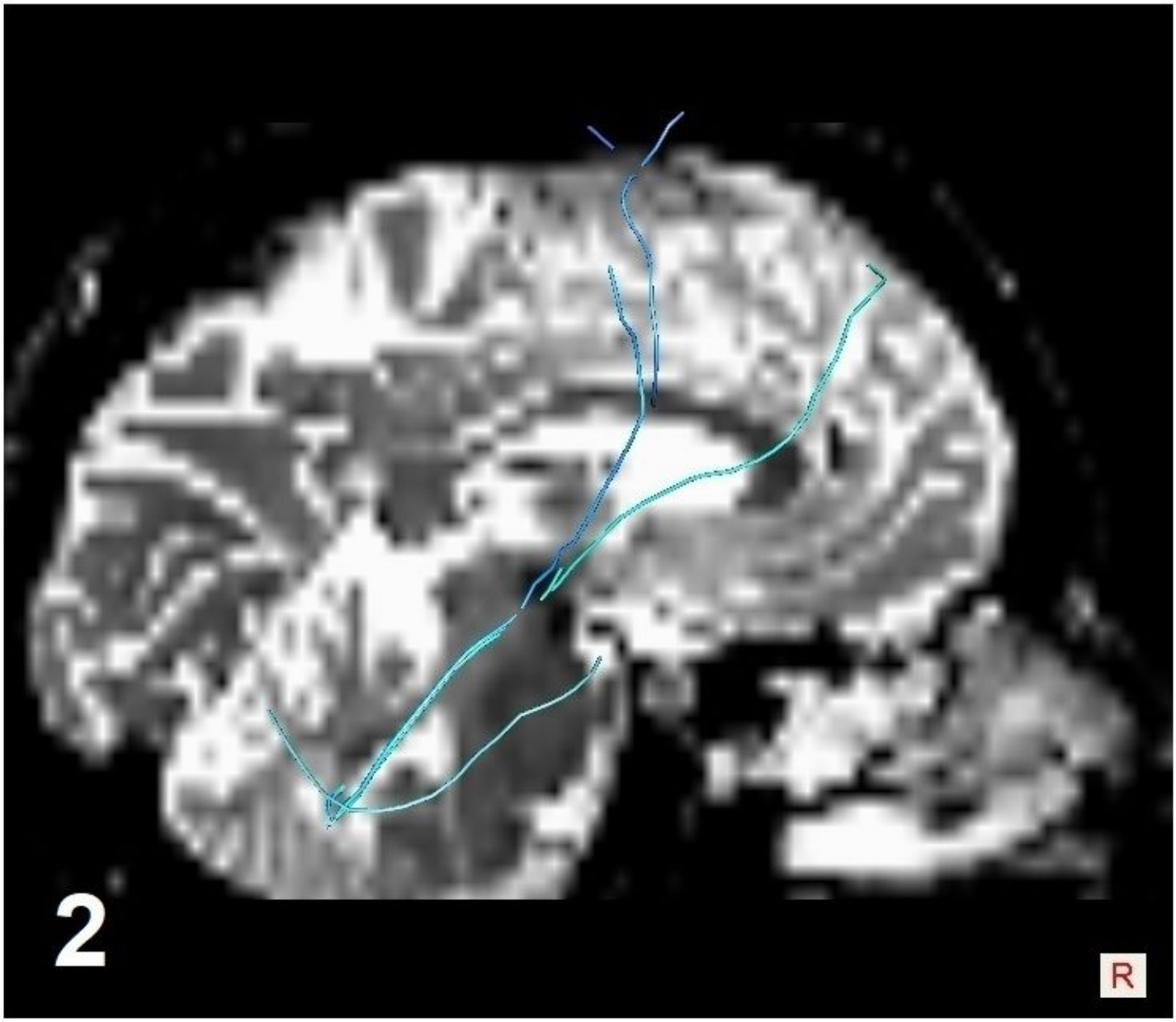

Figure 2

DSI-T2 fusion. Sagittal views. partially visible DRTT with a solitary fiber extending from ND to cerebral cortex.

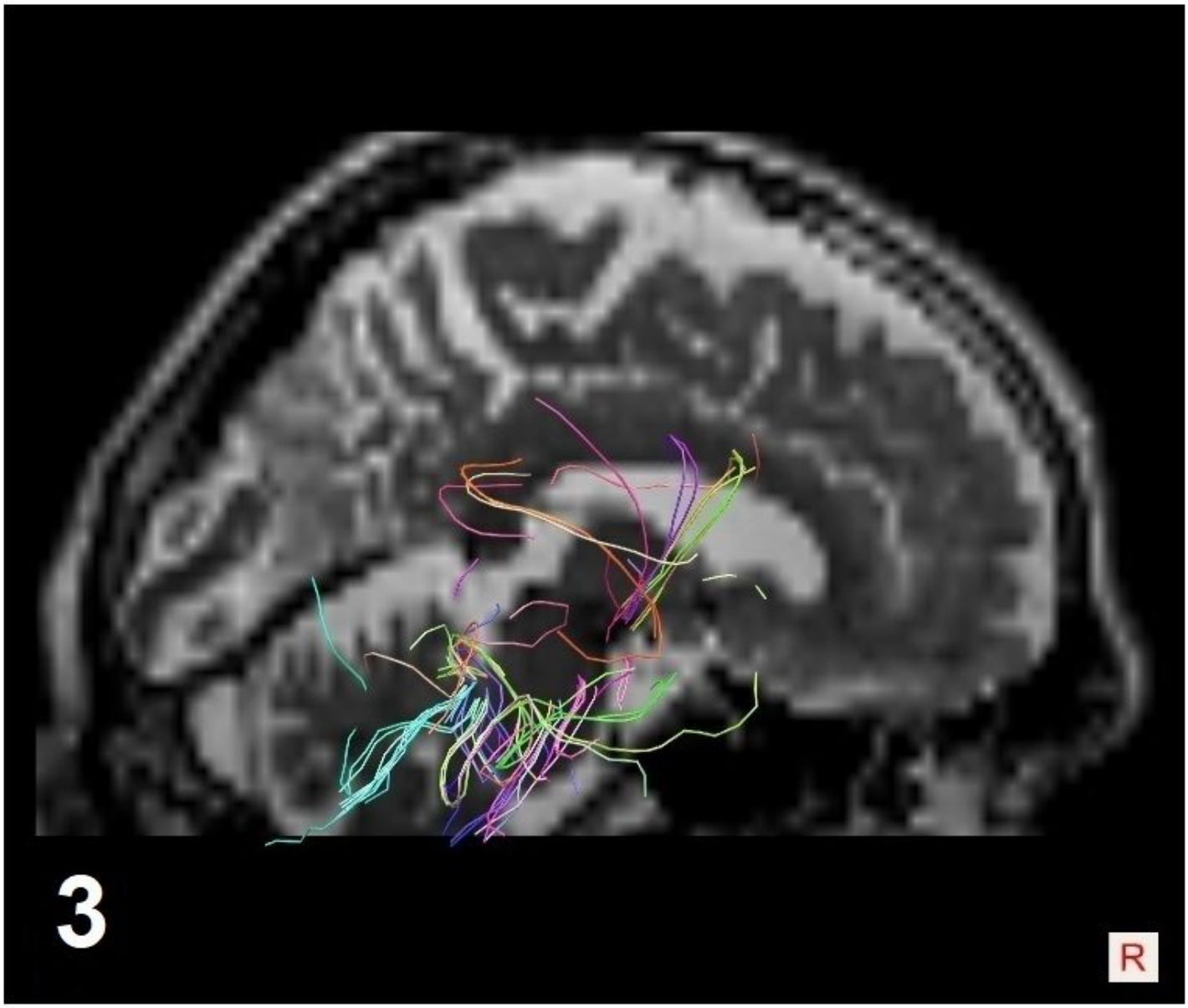

Figure 3

DSI-T2 fusion. Sagittal views. No DRTT-relevant structure of random fibers containing diffusion tensors that are not aligned (multicolour broken non harmonic fibers).

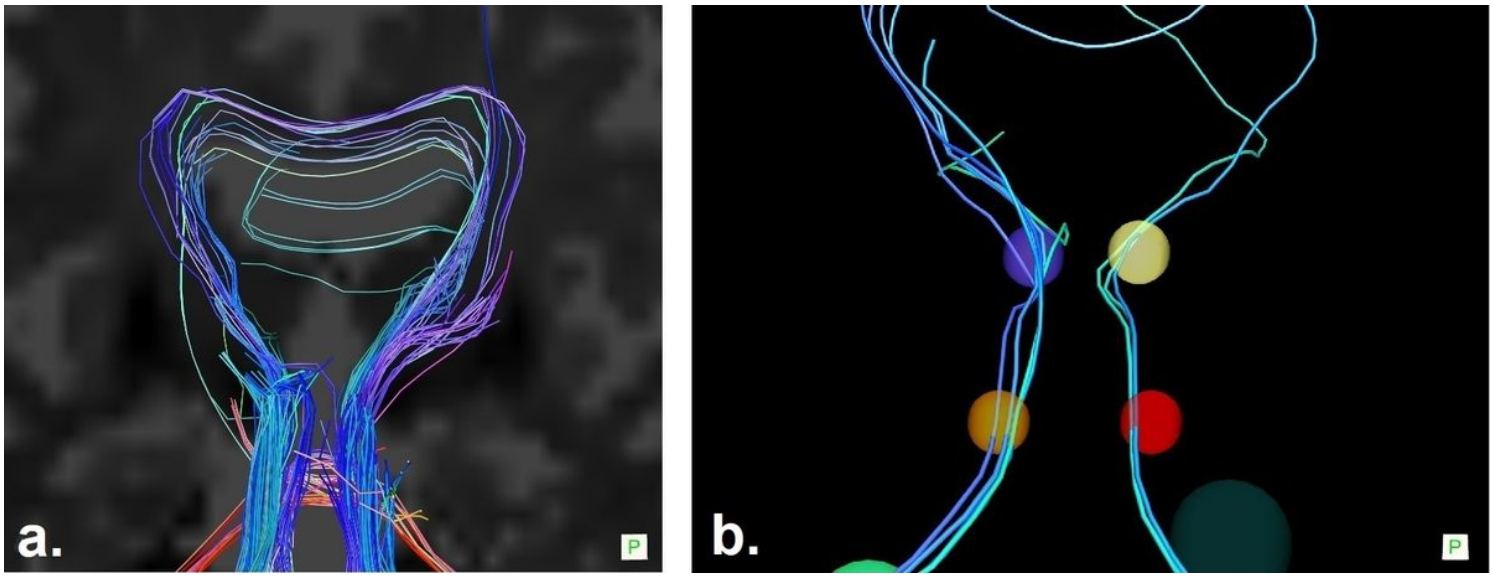

Figure 4

a DSI-T2 fusion. Coronal views. The blue and green fiber bundles (DRTT) on bottom of picture tend to move vertically but do not decussate. b Different case where the blue and green fibers on bottom of picture move symmetrically up to NR (purple and yellow ROIs) without crossing. Red, orange ROIs: superior cerebellar peduncle. Purple, yellow ROIs: nucleus ruber.

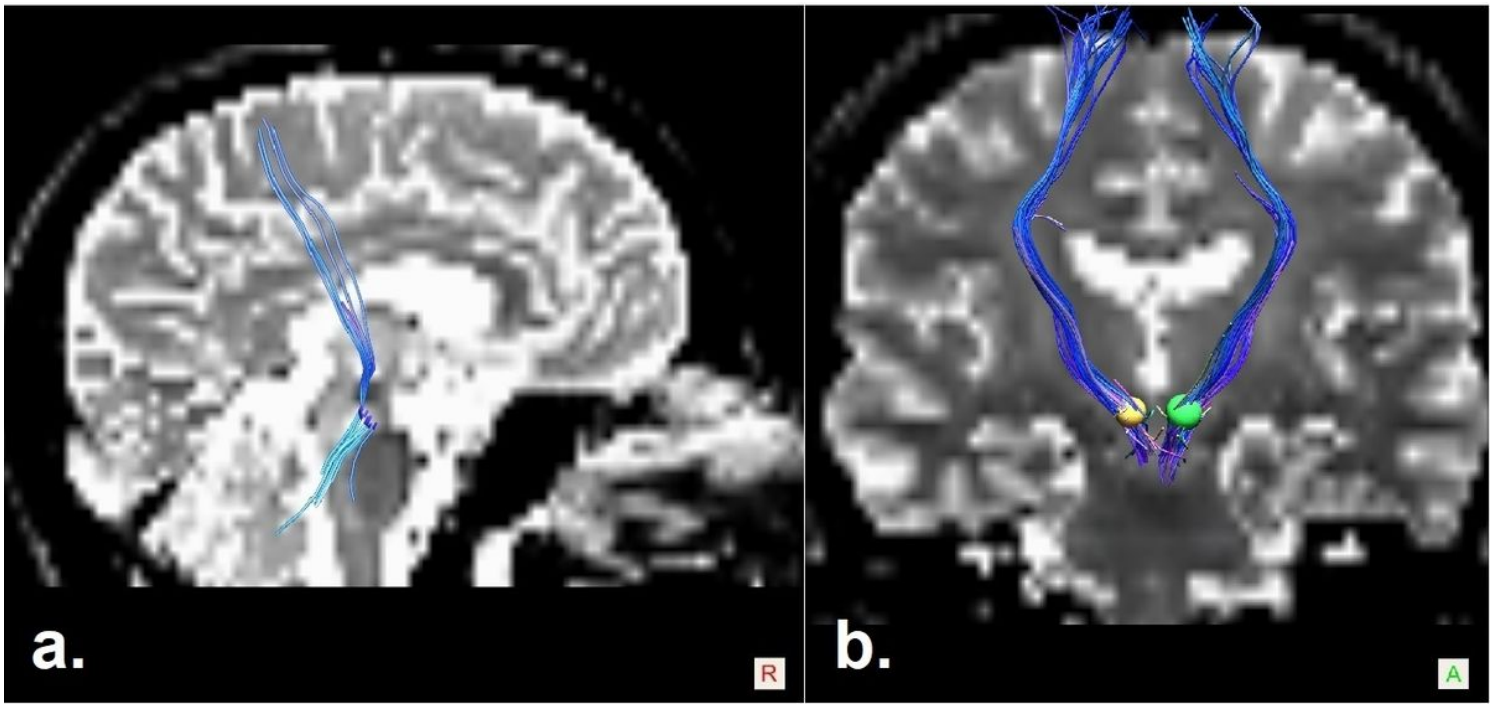

Figure 5

a DSI-T2 fusion. Sagittal view. Example of a successfully depicted DRTT tract b Coronal view of a successfully depicted DRTT tract. Green and yellow ROIs: nucleus ruber

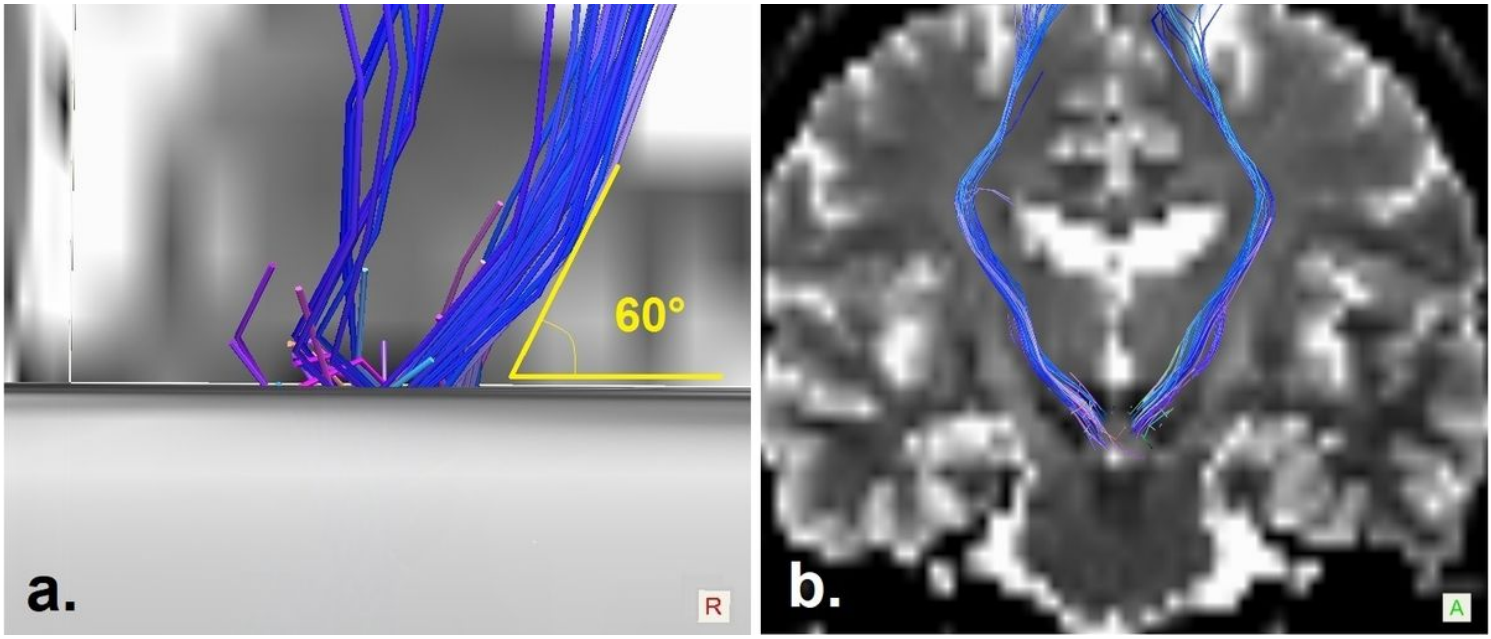

Figure 6

a DSI-T2 fusion. Sagittal close-up, angle based on sagittal axis. Axial plane level is 3mm inferior to AC PC. Note that as the tract ascends through the thalamus the angle increases above 60 degrees approaching nearly 80 degrees. b DSI-T2. Anteroposterior view of coronal plane at 6mm anterior to midcomissural level. Note the DRTT from NR and upwards and the crooked angling of the DRTT as it leaves NR.

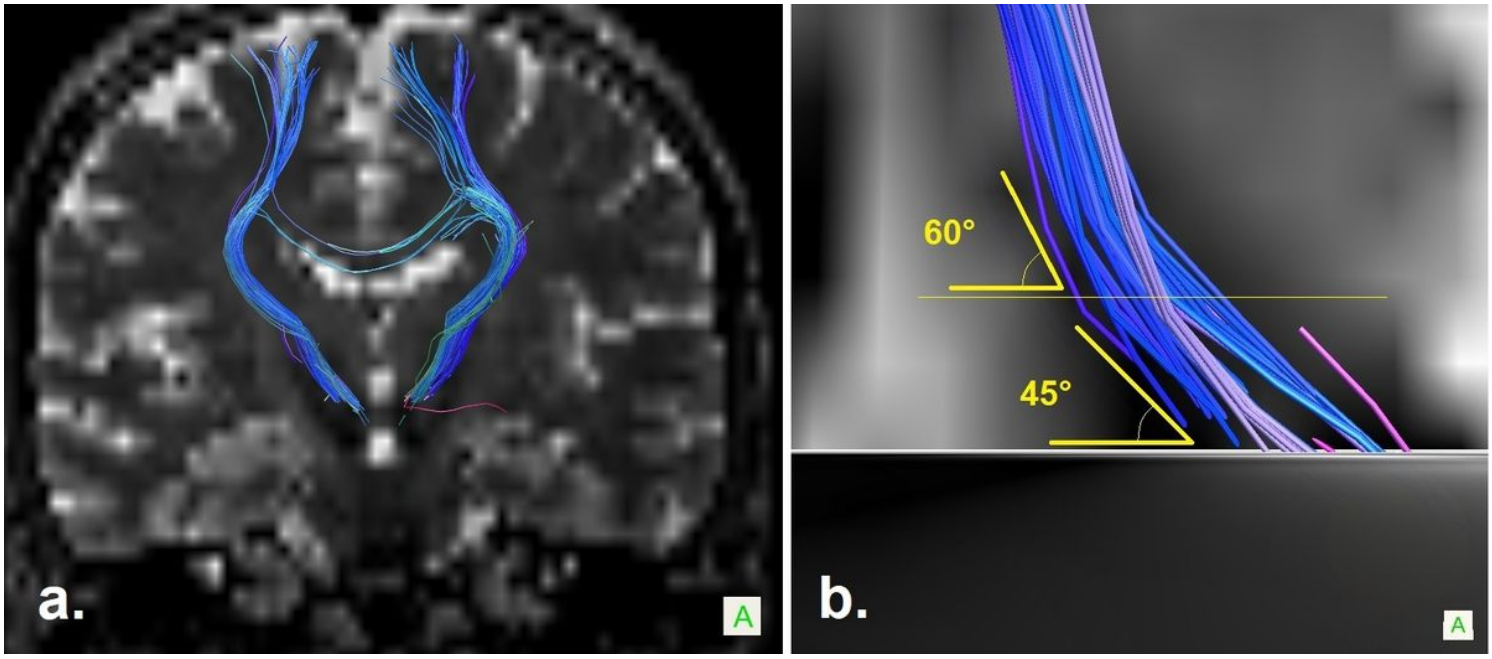

Figure 7

a DSI-T2 fusion. Anteroposterior view of coronal plane of DRTT from NR onwards. b Coronal close-up. Angle based on transverse axis. Axial plane 3mm inferior to AC PC.

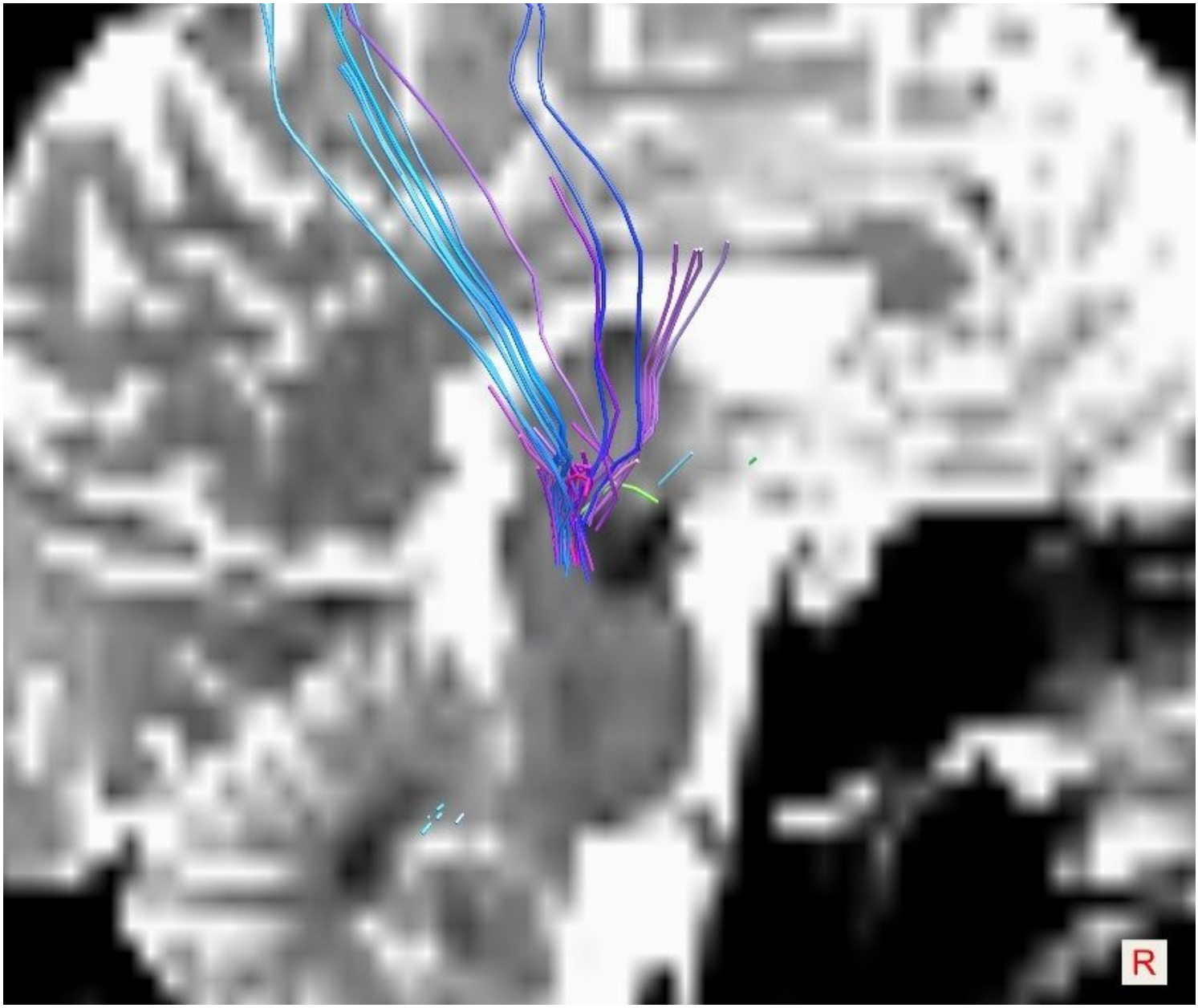

Figure 8

DSI-T2 fusion. Sagittal view. The cortical projections of DRTT are visible in a precentral distribution.

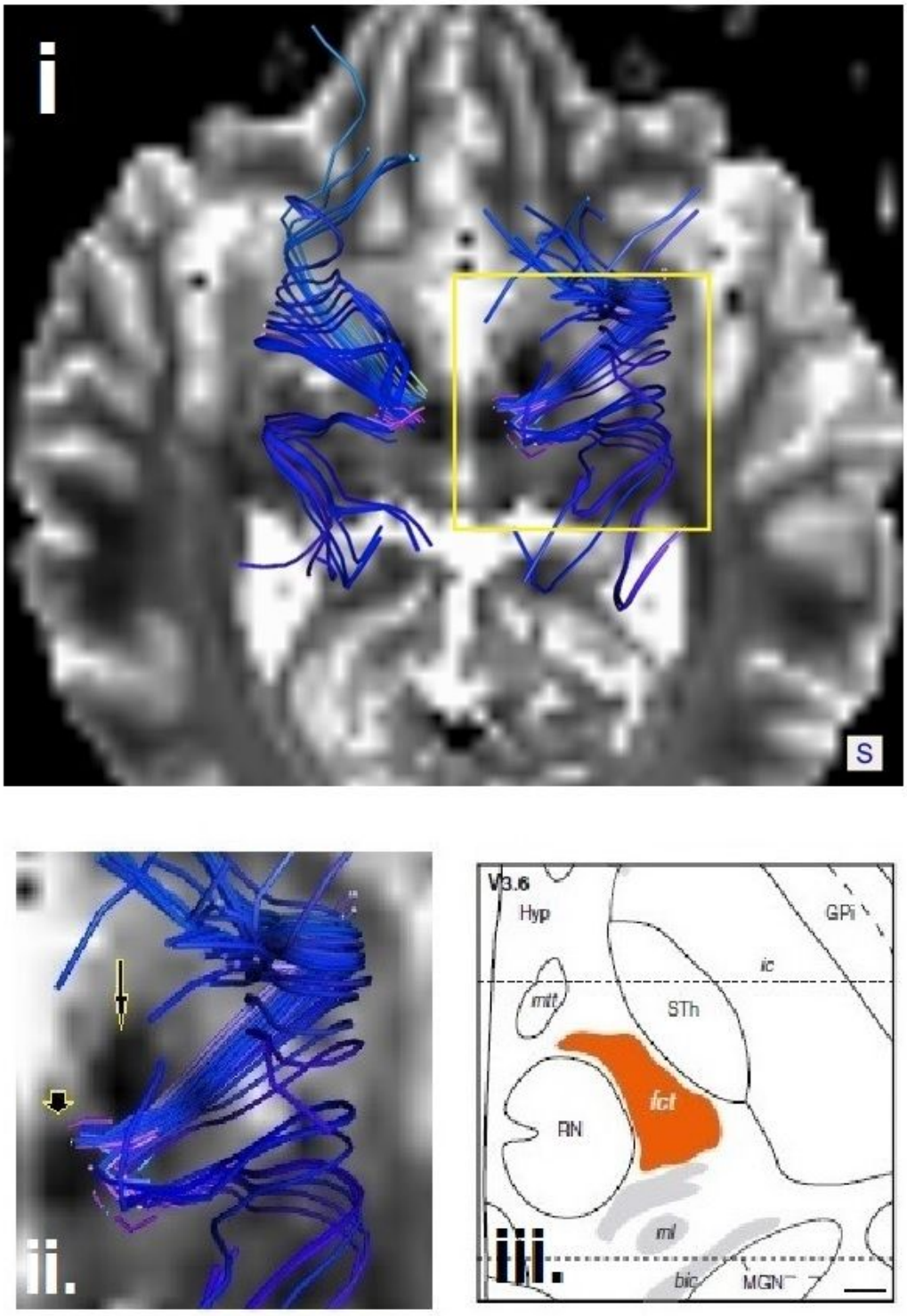

Figure 9

i. Modified axial plane, 3 mm inferior to intercommissural AC PC. plane. ii. Axial close-up; Axial plane 3mm inferior to AC PC. Short arrow: RN, long arrow: STh. iii. Modified axial atlas map, 3,6 mm inferior to AC PC. (adaptation/modification/after permission of Gallay et al (Gallay et al., 2008)).

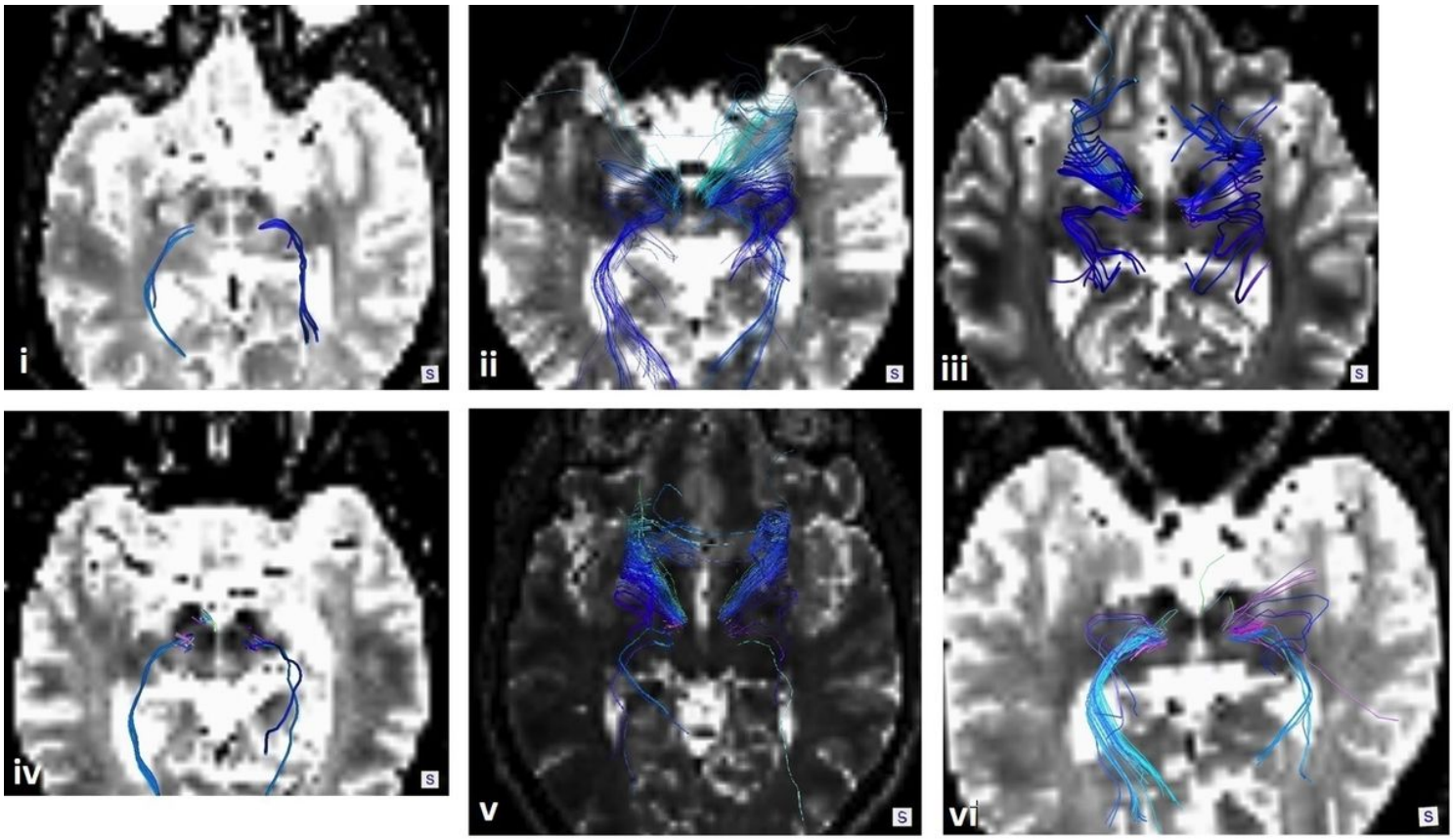

Figure 10

DSI-T2 fusion. Axial view at 3mm inferior to the intercommissural AC PC. plane in all of the successfully depicted DRTT tracts. Note the fibers emerging points related to NR and STh as well as the variability between i, iv, vi and ii, iii, v concerning the amount of fiber bundles.

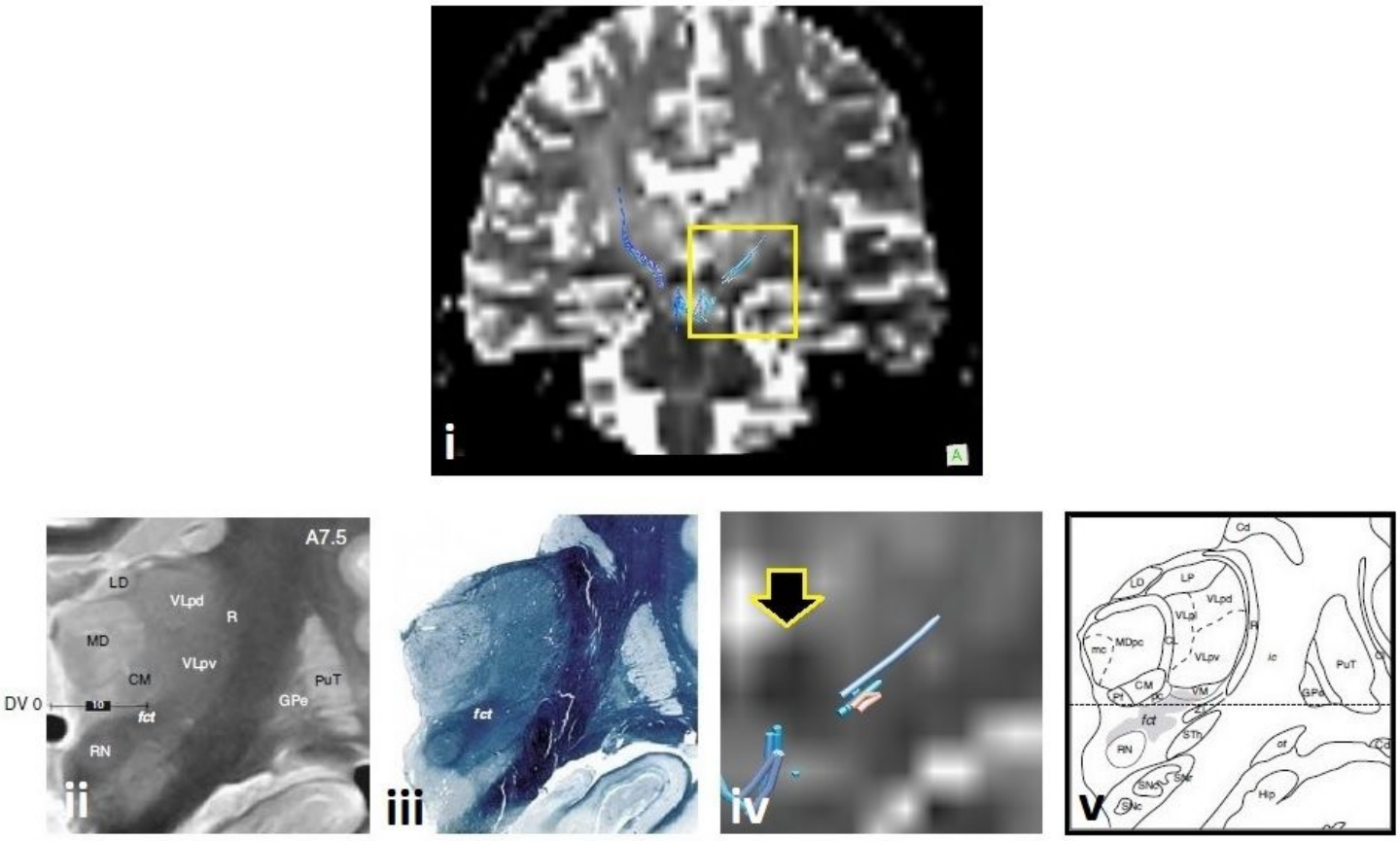

Figure 11

i.: DSI-T2 fusion. Coronal plane at 6,6 mm anterior to the PC level. ii- iii.: Modified images of : coronal view of proton density MRI, myelin section. iv.: DSI-T2 fusion. Coronal close up view of DRTT, at 6,6 mm anterior to the PC level. Short arrow: nucleus ruber (RN). v.: Atlas map at 7,5 mm anterior to the PC level. (adaptation/modification/courtesy of Gallay et al after permission (Gallay et al., 2008)).

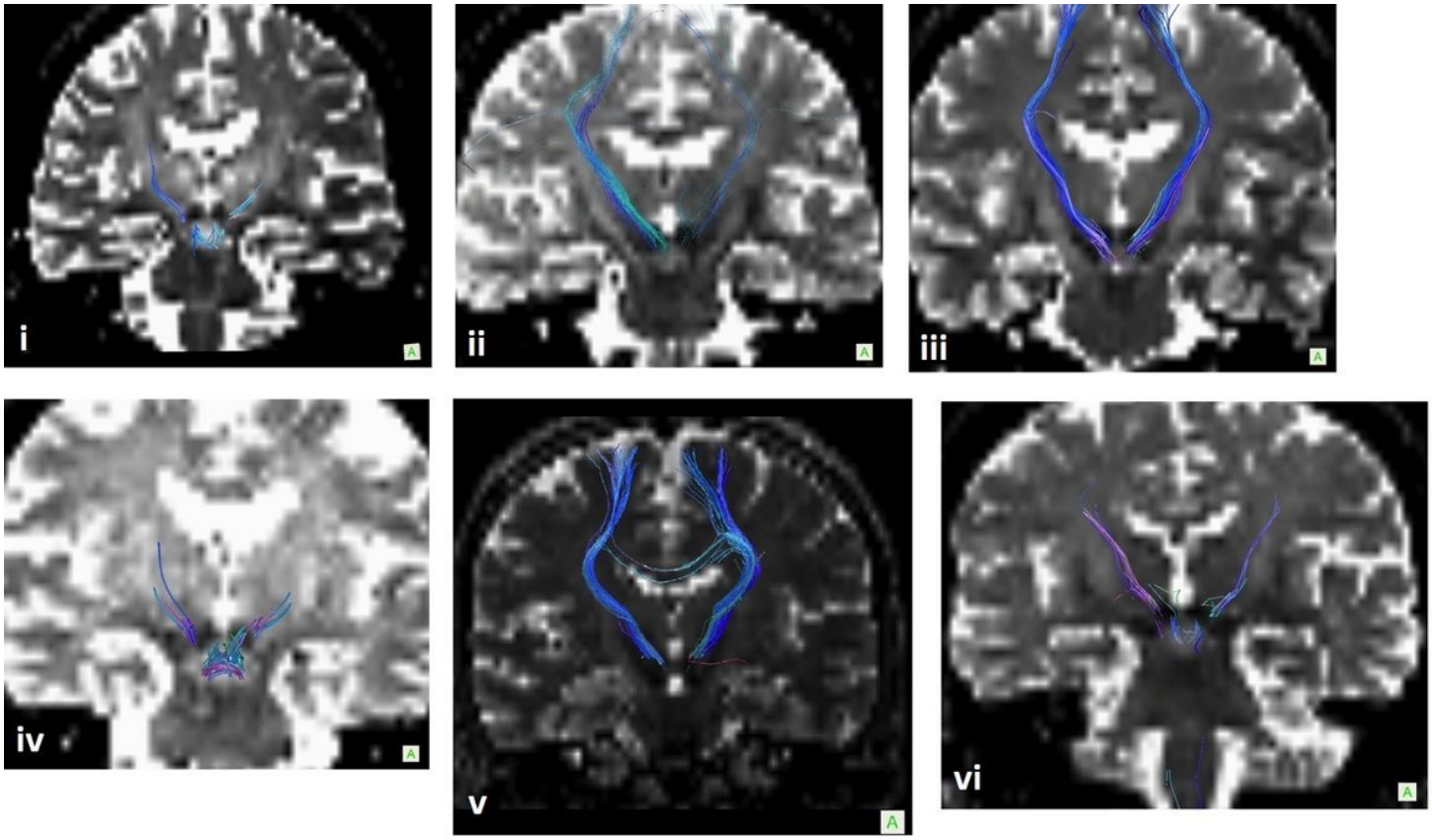

Figure 12

i- vi.: DSI-T2 fusion. Coronal view at 6,6 mm anterior to PC level in all of the successfully depicted DRTT tracts. Note the fibers' orientation passing lateral and inferior to NR then medial to STh.

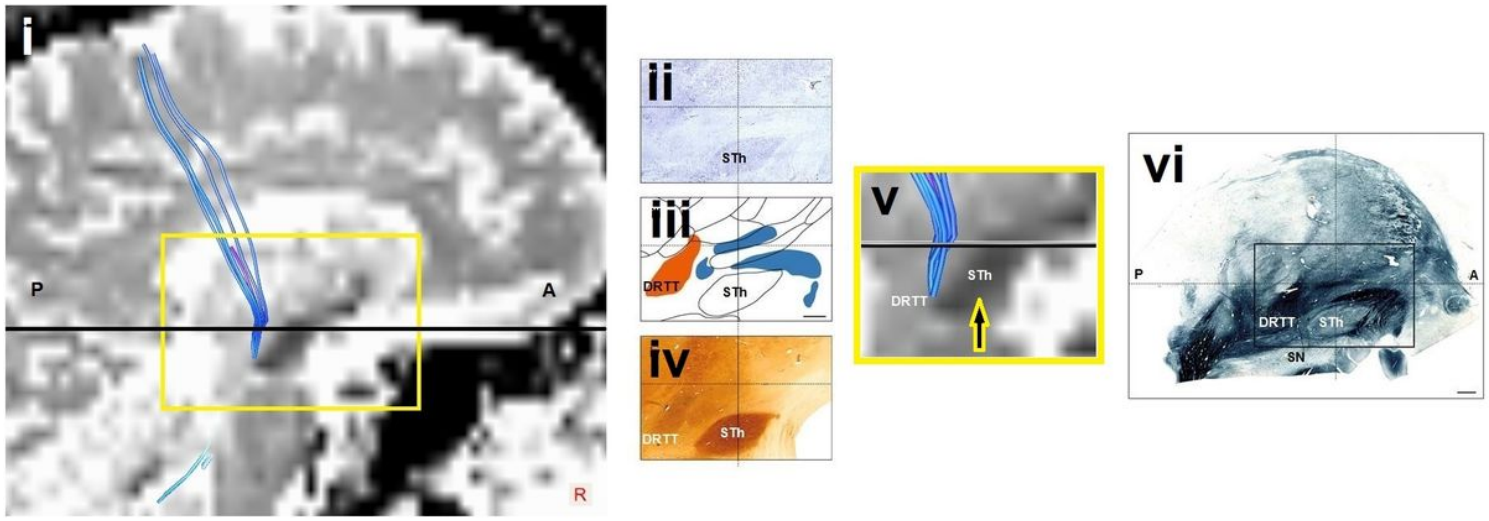

Figure 13

i- iv.: Sagittal views of DSI, Nissl section, atlas, PV immunostaining at 8,1 mm lateral to the intercommisural line. v.: Sagittal close-up view of DSI at 8,8 mm lateral. Fibers ascend posterior to the nucleus subthalamicus (long arrow). vi.: Myelin stained section at 8,1 mm lateral. DRTT:

dentatorubrothalamic tract, STh: nucleus subthalamicus, SN: substantia nigra. (adaptation/modification/ courtesy of Gallay et al (Gallay et al., 2008) after permission).

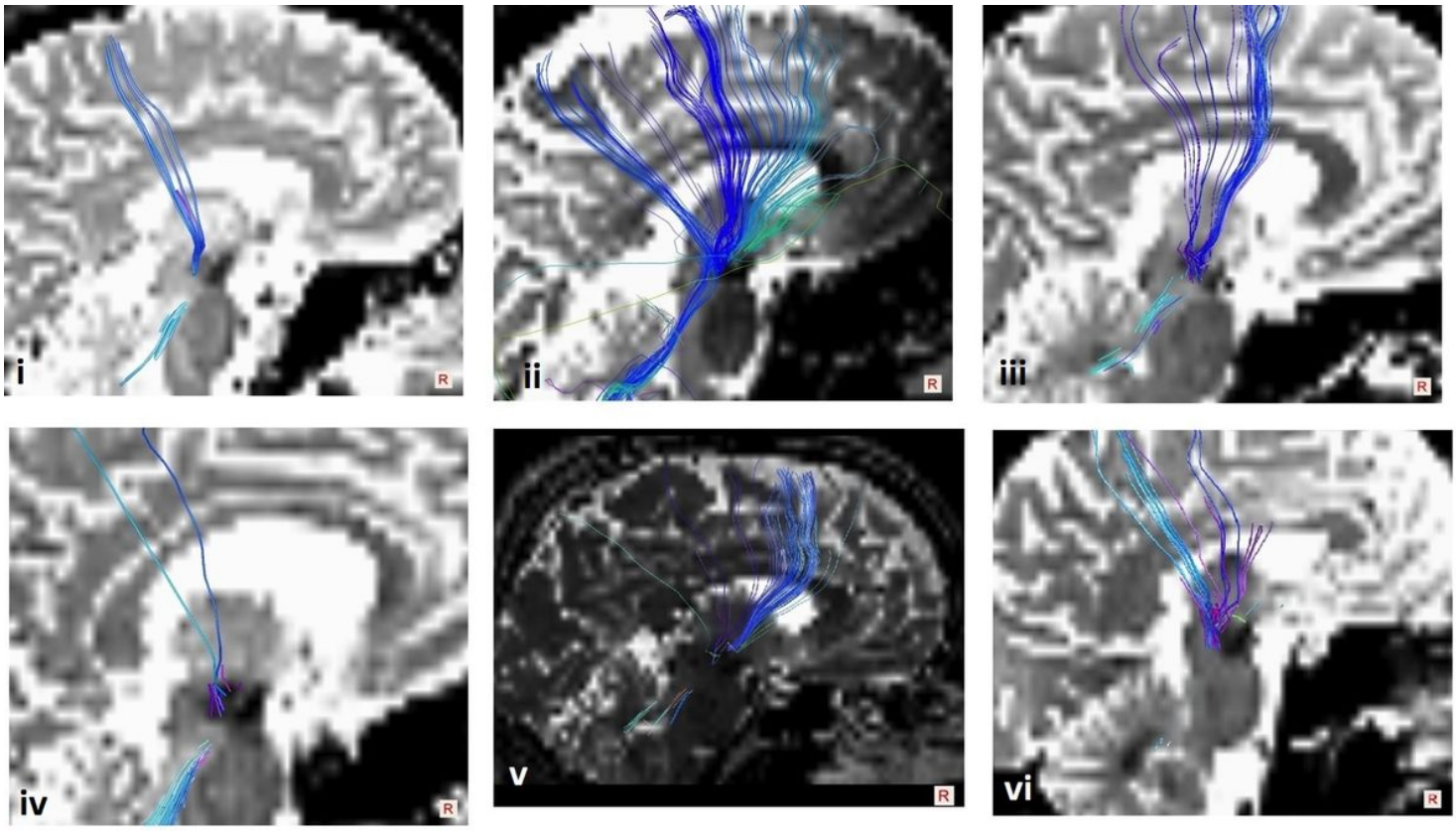

Figure 14

DSI-T2 fusion. Sagittal view at 6,6 mm lateral to the intercommissural line in all of the successfully depicted DRTT tracts. Note the course of DRTT consistently posterior and parallel to STh (hypointense mass in brainstem), moving vertical and curving slightly posterior after its intrathalamic course. Note also the variability among the images, regarding the amount of fiber bundles.